PRESSURE LOSSES IN SMALL-SIZED PARABOLIC-TROUGH SOLAR FIELDS FOR INDUSTRIAL PROCESS HEAT

Loreto Valenzuela[1], David Hernández-Lobón[2], Eduardo Zarza[2], Manuel Pérez[3]

[1] Plataforma Solar de Almería-CIEMAT, Crta. Senés, km.4, E04200 Tabernas, Almeria (Spain);

loreto.valenzuela@psa.es, +34 950387934

[2] Plataforma Solar de Almería-CIEMAT, Tabernas, Almería (Spain)

[3] CIESOL-Universidad de Almería, Almería (Spain)

1. Introduction

Using parabolic-trough solar collectors (PTC) for industrial thermal processes in the temperature range up to 300ºC is not new (Fernández-García et al., 2010), but in the last five years there is a boosted interest in this type of concentrating solar technology. The Capsol project was born under this framework with the objectives of design, developing, and testing a new PTC collector prototype (Fernández et al., 2010).

One of the problems that arise when designing PTC solar fields is how to deal with the pressure losses which are particularly critical when producing saturated steam. Depending on the industrial process, the specific heat demand and the inlet/outlet process fluid temperatures, a solar field configuration can be feasible or not. For the case study presented in this paper, a sensitive analysis of a small-sized PTCs solar field loop is performed. The PTC selected is the Capsol collector, which has a focal length of 0.2m and an aperture area of 2 m^2 (1mx2m), and its steel absorber pipe has an inner diameter of 15 mm. From the results obtained, it is possible to conclude which loop length and nominal working conditions would be optimal. The study has been done considering the production of pressurized hot water and saturated steam.

2. Methodology

The study is based on steady-state process modeling. This tackles the general problem of solving the behavior of a system of interconnected equipment units with streams of energy, momentum and mass between them. The tool has been developed in the software environment MatLab/Simulink® and allows simulating single-phase and two-phase parabolic-trough solar collectors system flows (Hernández et al., 2011).

The Capsol-PTC collector has a parabolic aluminum reflector surface which concentrates beam solar radiation on the absorber tube which is a fixed carbon steel tube located in the focal line of the parabola. The absorber tube is covered by a non-evacuated glass pipe. In the aperture plane of the parabola there is also a flat glass cover which improves structural stability and reduces maintenance requirements. The geometric, optical, and thermal characteristics of this solar collector are listed in Table 1.

Considering the data of the collector Capsol-PTC in Table 1, calculation of the effective thermal power in the collector has been done as follows:

$$\eta_{overall} = \frac{\dot{Q}_{useful}}{\dot{Q}_{solar}} \qquad \text{(eq. 1)}$$

where overall efficiency $\eta_{overall}$ in a solar collector is the ratio of useful thermal power transferred to the heat transfer fluid, $\dot{Q}_{useful}$, and the incident solar radiation on the collector, $\dot{Q}_{solar}$. Therefore the heat flow rate transferred to the fluid can be expressed as:

$$Q_{useful} = G_b \cdot \cos(\theta) \cdot K(\theta) \cdot A_{cap} \cdot \left(0.63 + 4 \cdot 10^{-4} \cdot \Delta T - 14 \cdot 10^{-6} \cdot \Delta T^2\right) \qquad \text{(eq. 2)}$$

where G_b is the direct normal irradiance (DNI) (in W/m^2), A_{cap} is the collector's aperture area (in m^2), $K(\theta)$ is the incidence angle modifier (dimensionless), and ΔT is the difference between the fluid's average temperature in the receiver and the ambient temperature (in ºC).

Tab. 1: Geometric, optical and thermal characteristics of the Capsol-PTC collector

Characteristic	Value or function
Aperture (m)	1.0
Length (m)	2.0
Absorber outer diameter (m)	0.018
Absorber inner diameter (m)	0.015
Absolute roughness of the pipe (m)	$50 \cdot 10^{-6}$
Peak optical-geometrical efficiency (-)	0.63
Incidence angle modifier (-)[1]	$K(\theta) = 1 - 1.63 \cdot 10^{-3} \cdot \theta - 4.64 \cdot 10^{-5} \cdot \theta^2$ (eq. 3)
Overall efficiency (-)[2]	$\eta_{overall} = 0.63 + 4 \cdot 10^{-4} \cdot \Delta T - 14 \cdot 10^{-6} \cdot \Delta T^2$ (eq. 4)

[1] The incidence angle is in degrees.

[2] ΔT is the difference between the fluid's average temperature in the receiver and the ambient temperature (in ºC).

Tab. 2: Nominal working conditions of the Capsol-PTC collectors' loop at the design point

Parameter	Value
Location	PSA, Tabernas (Latitude 37º05´28´´N, Longitude 2º21´19´´W)
Design date	June 21st, 12:00 (Solar time)
Direct normal irradiance (W/m²)	850
Ambient temperature (ºC)	25
Collectors axis orientation	North-South
Number of collectors per loop	38
Loop inlet pressure (MPa)	{1.0, 2.0}
Loop inlet temperature (ºC)	{90, 125}
Loop inlet mass flow (kg/s)	{0.01, 0.02}

The nominal working conditions selected for simulations were established selecting a possible industrial process heat (IPH) demand in terms of temperature/pressure levels, and considering a specific geographical location as well as a specific date and solar time to compute the incidence angle at the design point. Once these values were established, several configurations of collectors' loop were selected and simulations were performed to determine inlet water mass flows needed to achieve temperature/pressure requirements. Finally a loop length was established and nominal working conditions defined are those shown in Table 2.

For this study, it was considered that mirrors were completely clean with a reflectance value equal to the nominal one (0.88). This value is included in the peak optical-geometrical efficiency (see Table 1).

The assumptions considered to calculate the pressure drop and heat losses in the interconnections between collectors within the loop are: a) the collectors' loop has a U form; and b) collectors in the line are coupled just one after another but c) in the interconnection between the two lines of the U loop there are 10 elbows of 90º and a straight pipe of 4m-length.

3. Sensitivity analysis

Sensitivity analysis has been performed changing different process parameters, i.e. working pressure, mass flow rate, inlet water temperature, DNI, and incidence angle. Pressure losses in the collectors' loop and steam fraction at the outlet have been obtained in these analyses to compare different process conditions.

3.1. Inlet pressure

The first parameter that was varied to study the evolution of pressure drop in the collectors' loop was the feedwater pressure at the entrance of the loop. Pressure values chosen were 1.0, 1.5, 2.0 and 2.5 MPa. Other working conditions were those listed in Table 2.

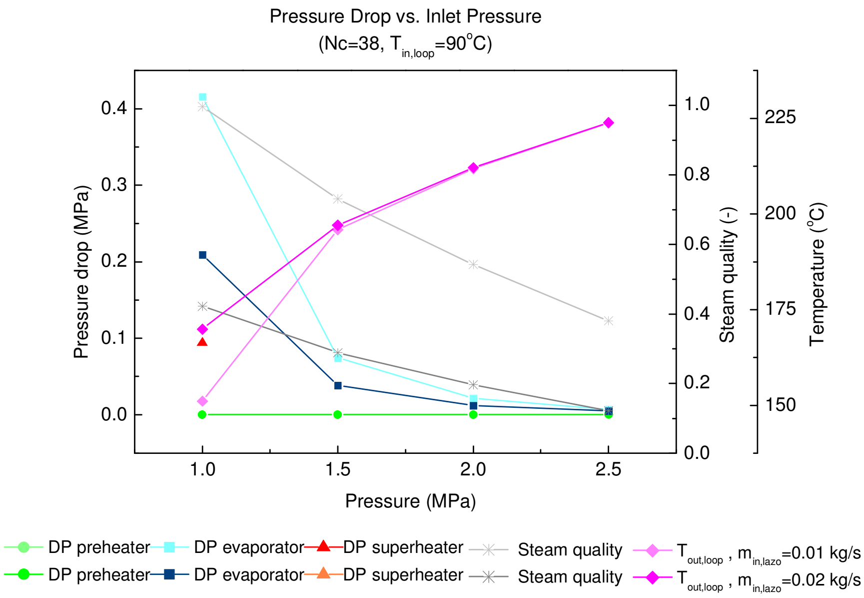

a)

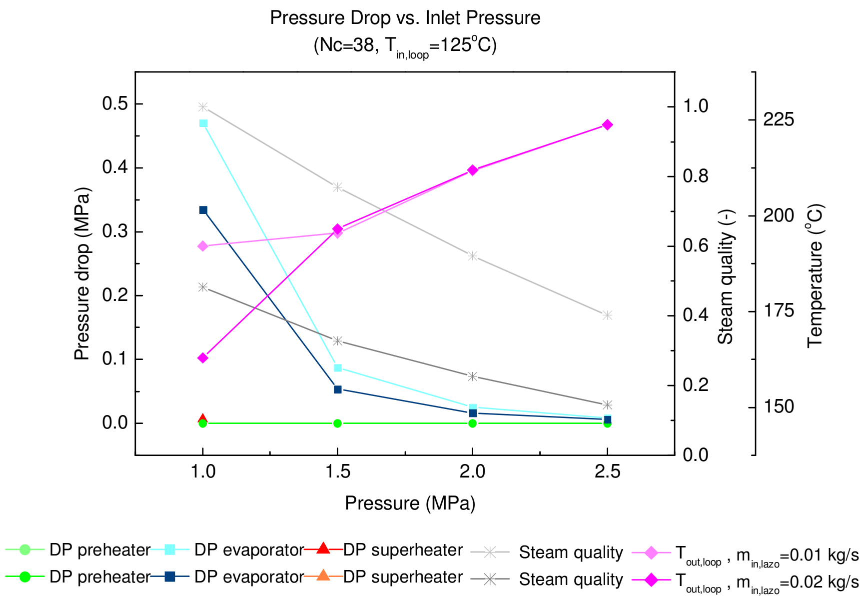

b)

Figure 1. Pressure drop versus inlet pressure in the collectors' loop:
a) feed water temperature of 90 ºC, b) feed water temperature of 125ºC.

Figure 1.a) includes the results corresponding to an inlet water temperature of 90ºC. In this case study steam fraction at the collectors' loop outlet is equal to 1 only when inlet mass flow is 0.01 kg/s and inlet pressure is 1 MPa. With these process conditions, pressure drop in the whole loop is higher than 0.5 MPa, which is around a 50% of the inlet pressure, and superheated steam temperature in the outlet is only 151ºC. Figure 1 shows the pressure drop in the three consecutive sections of the collectors' loop (water preheating,

evaporation and steam superheating), so that the total pressure drop for every case study is the sum up of these three values. Inlet pressure values of 1.5 MPa and 2.0 MPa gives steam fractions higher than 0.5 and pressure losses in the loop are smaller than 0.1 MPa. With an inlet pressure of 2.5 MPa, the steam fraction at the outlet is only 0.38 but pressure drop is quite small, less than 0.01 MPa, therefore the outlet two-phase-fluid temperature is 224ºC. When inlet mass flow is 0.02 kg/s, steam fraction at the outlet varies from 0.42, when inlet pressure is 1.0 MPa, to 0.12, for 2.5 MPa; and outlet fluid temperature varies from 170ºC to 224ºC in the pressure range considered. According to these values, pressure losses are only significant when inlet pressure is 1 MPa. In all cases analyzed, pressure drop in the preheating section is not relevant compared to pressure losses in evaporation or superheating sections.

Tab. 3: Pressure drops in the preheating, evaporation and superheating sections of the collectors' loop, outlet steam fraction and outlet fluid temperature as a function of the inlet fluid pressure in the Capsol-PTC collectors' loop

T_{in} (ºC)	P_{in} (MPa)	ΔP_{pre} (MPa)	ΔP_{eva} (MPa)	ΔP_{sup} (MPa)	X_{out} (-)	T_{out} (ºC)	ΔP_{pre} (MPa)	ΔP_{eva} (MPa)	ΔP_{sup} (MPa)	X_{out} (-)	T_{out} (ºC)
		$\dot{m}_{in}$ =0.01kg/s					$\dot{m}_{in}$ =0.02 kg/s				
90	1.0	4E-05	0.5101	-	0.98	151	0.0003	0.2092	-	0.42	170
	1.5	6E-05	0.0746	-	0.73	196	0.0004	0.0383	-	0.29	197
	2.0	8E-05	0.0217	-	0.54	212	0.0005	0.0120	-	0.20	212
	2.5	9E-05	0.0071	-	0.38	224	0.0006	0.0052	-	0.12	224
125	1.0	3E-05	0.4711	0.0064	1.00	192	0.0002	0.3347	-	0.48	163
	1.5	4E-05	0.0874	-	0.77	195	0.0003	0.0538	-	0.33	197
	2.0	6E-05	0.0253	-	0.57	212	0.0004	0.0162	-	0.23	212
	2.5	8E-05	0.0082	-	0.40	224	0.0005	0.0066	-	0.14	224

3.2. Inlet mass flow rate

The second parameter that was varied to study the evolution of pressure drop in the system was the feedwater mass flow rate of the collectors' loop. Flow rates chosen were 0.01 kg/s, 0.015 kg/s, 0.02 kg/s and 0.025 kg/s. Two values of feed water temperature, 90ºC and 125 ºC, and two working pressures, 1.0 MPa and 2.0 MPa, were considered. In addition the nominal working conditions defined in Table 2 were used.

The effect of the inlet mass flow on the total pressure losses in the collectors' loop can be seen in Table 4.

Tab. 4: Pressure drops in the preheating, evaporation and superheating sections of the collectors' loop, outlet steam fraction and outlet fluid temperature as a function of the feed water mass flow rate in the Capsol-PTC collectors' loop

P_{in} (MPa)	$\dot{m}_{in}$ (kg/s)	ΔP_{pre} (MPa)	ΔP_{eva} (MPa)	ΔP_{sup} (MPa)	X_{out} (-)	T_{out} (ºC)	ΔP_{pre} (MPa)	ΔP_{eva} (MPa)	ΔP_{sup} (MPa)	X_{out} (-)	T_{out} (ºC)
		T_{in} = 90ºC					T_{in} = 125ºC				
1.0	0.010	4E-5	0.5101	-	0.98	151	3E-5	0.4711	0.0064	1.00	192
	0.015	0.0001	0.2999	-	0.61	165	8E-5	0.4530	-	0.68	155
	0.020	0.0003	0.2092	-	0.42	170	0.0002	0.3347	-	0.48	163
	0.025	0.0006	0.1550	-	0.31	173	0.0004	0.2687	-	0.37	167
2.0	0.010	8E-5	0.0217	-	0.54	212	6E-5	0.0253	-	0.57	212
	0.015	0.0002	0.0152	-	0.31	212	0.0001	0.0193	-	0.34	212
	0.020	0.0005	0.0120	-	0.20	212	0.0004	0.0162	-	0.23	212
	0.025	0.0010	0.0105	-	0.13	212	0.0008	0.0148	-	0.16	212

Figure 2.a) includes the results corresponding to an inlet water pressure of 1.0 MPa. In this case study steam fraction at the collector loop outlet is equal to 1 only when inlet mass flow is 0.01 kg/s and inlet water temperature is 125ºC. With these process conditions, pressure drop in the whole loop is 0.48 MPa, which is about 50% of the inlet pressure, and superheated steam temperature at the outlet is 192ºC. When inlet water temperature is 90ºC, steam fraction varies from 0.98 for a mass flow rate of 0.01 kg/s to 0.31 for a mass flow rate of 0.025 kg/s. Pressure drop is 0.51 MPa for 0.01 kg/s and 0.16 MPa for 0.025kg/s. When inlet water temperature is 125ºC, steam fraction varies from 1.0 for mass flow rate of 0.01kg/s to 0.37 for a flow rate of 0.025 kg/s. Total pressure drop is 0.48 MPa for 0.01 kg/s and 0.27 MPa for 0.025kg/s.

Figure 2.b) includes the results corresponding to an inlet water pressure of 2.0 MPa. In this case study, steam fraction at the outlet varies within the range 0.1 to 0.6 for the two inlet water temperature values considered. Pressure losses are higher when steam fraction is near 0.6, but they are within the range of 0.022 to 0.025 MPa (about 1% of the inlet fluid pressure).

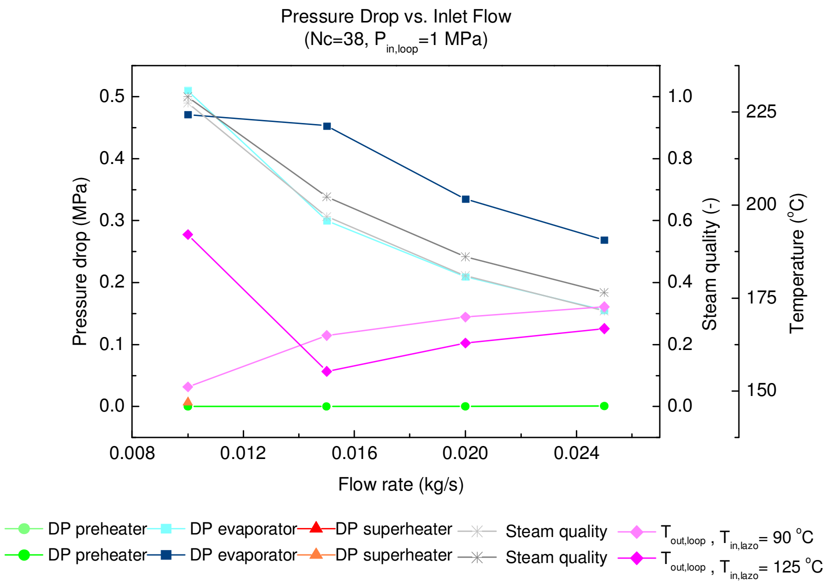

a)

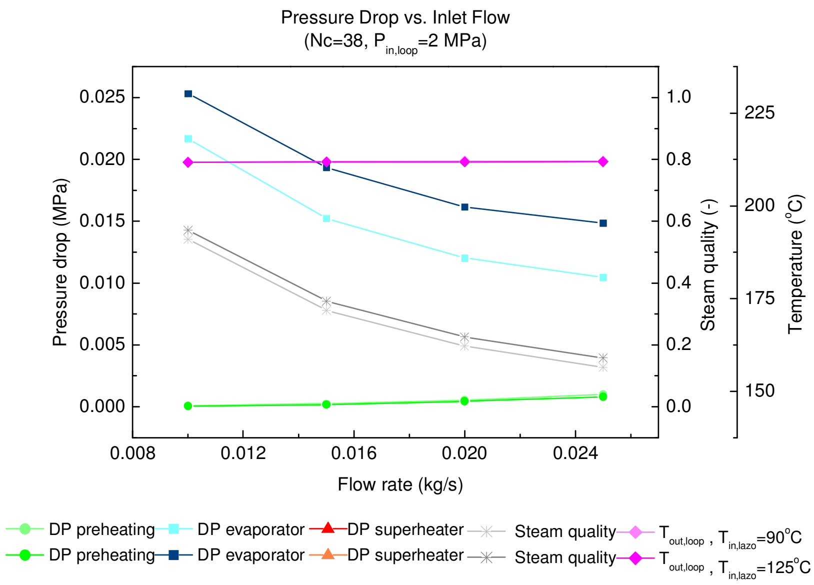

b)

Figure 2. Pressure drop versus inlet mass flow in the collectors' loop:
a) inlet pressure of 1 MPa, b) inlet pressure of 2 MPa.

3.3. Inlet temperature

For this case study, subcooled water temperatures considered for the collectors' loop entrance were: 80ºC, 100ºC, 120ºC, and 140ºC. Two working pressures were selected, 1.0 MPa and 2.0 MPa. Additionally, mass flow rates considered were 0.01 kg/s and 0.02 kg/s.

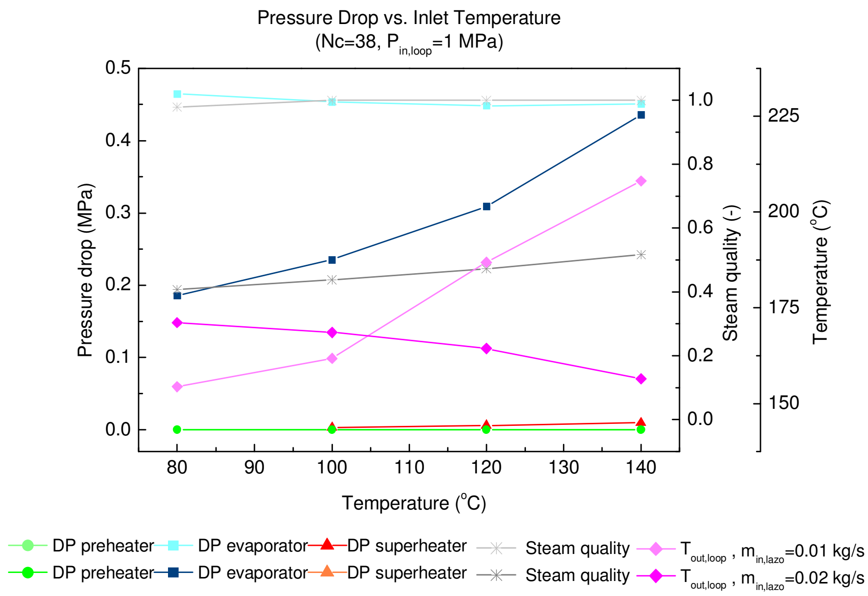

a)

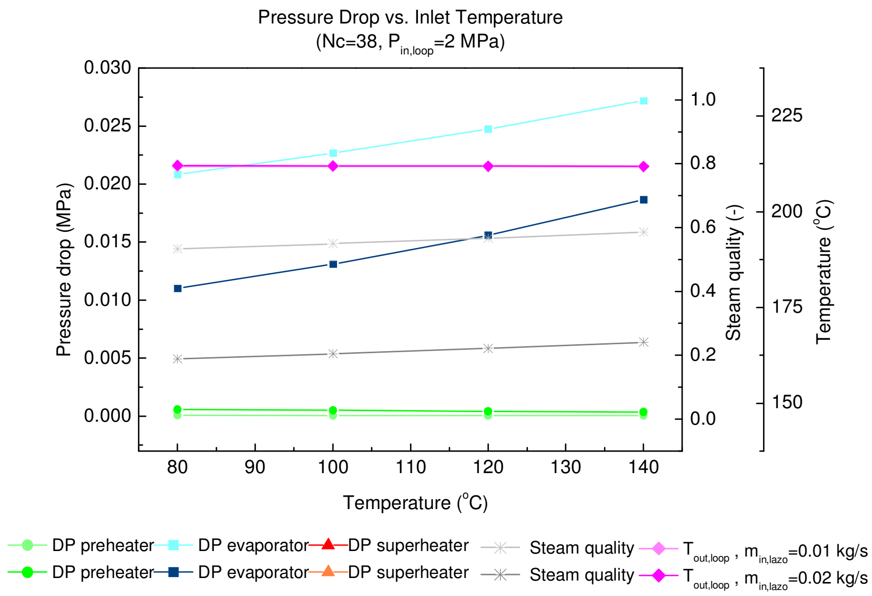

b)

Figure 3. Pressure drop versus inlet fluid temperature in the collectors' loop: a) inlet pressure of 1 MPa, b) inlet pressure of 2 MPa.

Figure 3.a) includes the results corresponding to an inlet working pressure of 1.0 MPa. In this case study steam fraction at the collectors' loop outlet is equal to 1 when inlet mass flow is 0.01 kg/s in almost all inlet water temperature values considered. With these process conditions, pressure losses in the whole loop are around 0.46 MPa and superheated steam temperature varies from 162ºC, when inlet water temperature is 100ºC, to 208ºC, when inlet temperature is 140ºC. Outlet steam fraction varies from 0.41 to 0.52 when inlet mass flow rate is 0.02 kg/s, and pressure losses in the collectors' loop varies from 0.19 MPa to 0.44 MPa.

Figure 3.b) includes the results corresponding to an inlet working pressure of 2.0 MPa. In this case study steam fraction is in the range of 0.5 when mass flow rate is 0.01 kg/s, and is in the range of 0.2 when mass flow rate is 0.02 kg/s. With these process conditions, pressure losses in the whole loop are in the range of 0.02 MPa when mass flow rate is 0.01 kg/s, and is in the range from 0.01 to 0.018 MPa when mass flow rate is 0.02 kg/s. As pressure losses are relatively small compared to the inlet working pressure, the outlet water-steam mixture temperature is 212ºC in all cases.

The pressure losses and outlet water-steam temperatures resulting from the analysis can be seen in Table 5.

Tab. 5: Pressure drops in the preheating, evaporation and superheating sections of the collectors' loop, outlet steam fraction and outlet fluid temperature as a function of the inlet fluid temperature in the Capsol-PTC collectors' loop

P_{in} (MPa)	T_{in} (ºC)	ΔP_{pre} (MPa)	ΔP_{eva} (MPa)	ΔP_{sup} (MPa)	X_{out} (-)	T_{out} (ºC)	ΔP_{pre} (MPa)	ΔP_{eva} (MPa)	ΔP_{sup} (MPa)	X_{out} (-)	T_{out} (ºC)
		$\dot{m}_{in}$ =0.01kg/s					$\dot{m}_{in}$ =0.02 kg/s				
1.0	80	5E-5	0.4651	-	0.98	154	0.0003	0.1859	-	0.41	171
	100	4E-5	0.4540	0.0031	1.00	162	0.0003	0.2355	-	0.44	169
	120	3E-5	0.4484	0.0061	1.00	187	0.0002	0.3092	-	0.47	164
	140	2E-5	0.4508	0.0094	1.00	208	0.0002	0.4359	-	0.52	156
2.0	80	8E-5	0.0208	-	0.53	212	0.0006	0.0110	-	0.19	212
	100	7E-5	0.0227	-	0.55	212	0.0005	0.0131	-	0.20	212
	120	6E-5	0.0248	-	0.57	212	0.0004	0.0156	-	0.22	212
	140	5E-5	0.0272	-	0.59	212	0.0004	0.0187	-	0.24	212

3.4. Direct normal irradiance

The fourth parameter considered in the sensitivity analysis was the direct normal irradiance on the collectors' aperture that influences the evolution of pressure drop in the collectors' loop and the steam fraction or superheated steam temperature at the outlet. DNI values chosen were 450 W/m^2, 600 W/m^2, 750 W/m^2 and 900 W/m^2. The feed water temperature considered was 90ºC, inlet mass flow rates were 0.01 kg/s and 0.02 kg/s, and other working conditions are listed in the Table 2.

The pressure losses and outlet fluid temperatures resulting from the analysis can be seen in Table 6.

Tab. 6: Pressure drops in the preheating, evaporation and superheating sections of the collectors' loop, outlet steam fraction and outlet fluid temperature as a function of the direct normal irradiance in the Capsol-PTC collectors' loop

P_{in} (MPa)	*DNI* (W/m^2)	ΔP_{pre} (MPa)	ΔP_{eva} (MPa)	ΔP_{sup} (MPa)	X_{out} (-)	T_{out} (ºC)	ΔP_{pre} (MPa)	ΔP_{eva} (MPa)	ΔP_{sup} (MPa)	X_{out} (-)	T_{out} (ºC)
		$\dot{m}_{in}$ =0.01kg/s					$\dot{m}_{in}$ =0.02 kg/s				
1.0	450	8E-5	0.0573	-	0.44	177	0.0006	0.0243	-	0.15	179
	600	7E-5	0.1366	-	0.64	174	0.0005	0.0617	-	0.25	177
	750	5E-5	0.2887	-	0.84	166	0.0004	0.1323	-	0.35	174
	900	4E-5	0.4571	0.0064	1.00	203	0.0003	0.2618	-	0.46	167
2.0	450	0.0001	0.0039	-	0.22	212	0.0010	0.0023	-	0.03	212
	600	0.0001	0.0085	-	0.34	212	0.0008	0.0050	-	0.10	212
	750	9E-5	0.0155	-	0.46	212	0.0006	0.0088	-	0.16	212
	900	7E-5	0.0253	-	0.58	212	0.0005	0.0140	-	0.22	212

Figure 4.a) shows the results for an inlet pressure of 1 MPa and two mass flow rates. When mass flow rate is 0.01 kg/s, superheated steam is generated only when DNI is 900 W/m^2 and pressure losses are 0.47 MPa in this case. For lower DNI values, steam fraction at the outlet varies from 0.11 when DNI is 450 W/m^2, to 0.84 when DNI is 750 W/m^2, and pressure losses in the evaporation section go from 0.06 MPa to 0.29 MPa, five times higher when DNI is 900 W/m^2. When mass flow rate is 0.02 kg/s, the steam fraction varies from 0.15 when DNI is 450 W/m^2, to 0.46 when DNI is 900 W/m^2, and pressure losses in the evaporation section range from 0.025 MPa to 0.26 MPa, ten times higher when DNI is 900 W/m^2. This fact causes the outlet fluid temperature to be higher when DNI is lower, 179ºC when DNI is 450 W/m^2 and 167ºC when DNI is 900 W/m^2.

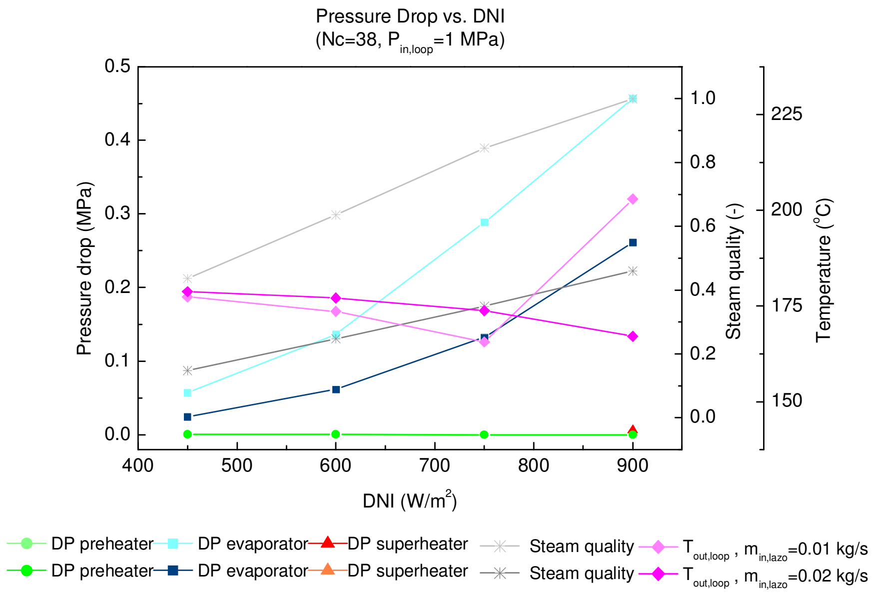

a)

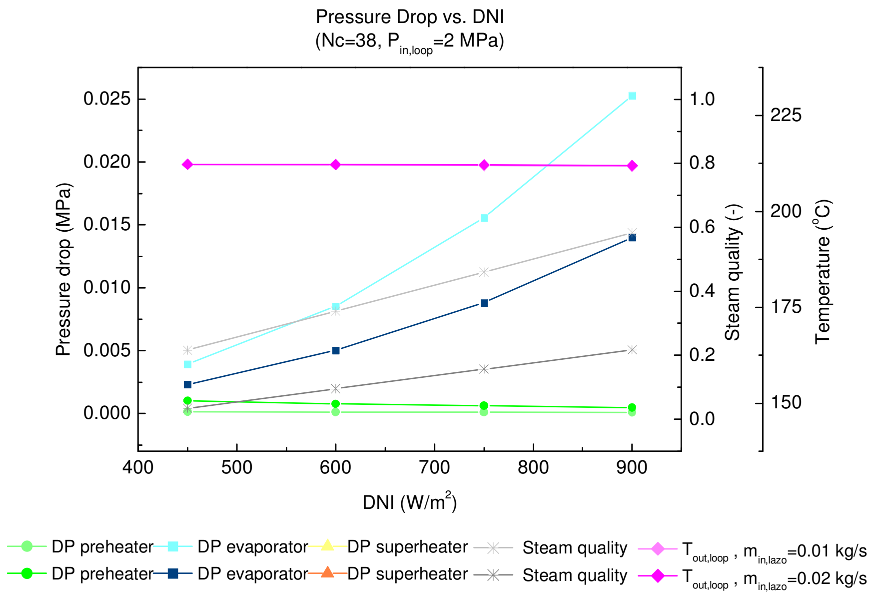

b)

Figure 4. Pressure drop versus direct normal irradiance in the collectors' loop: a) inlet pressure of 1 MPa, b) inlet pressure of 2 MPa.

3.5. Incidence angle

Finally, keeping DNI constant, the incidence angle was varied to analyze its influence on pressure losses. Results expected were similar to those obtained varying DNI, but we have included this section to show how pressure losses change even with a complete sunny day but due to the movement of the sun from the sunrise to sunset. Incidence angles chosen for this case study were reduced to the following values: 0º, 15º and 30º. Keep in mind that the collectors' loop is oriented in North-South direction. Feed water temperature was 90ºC and two mass flow rates were again considered, 0.01 kg/s and 0.02 kg/s. Other working conditions are listed in Table 2.

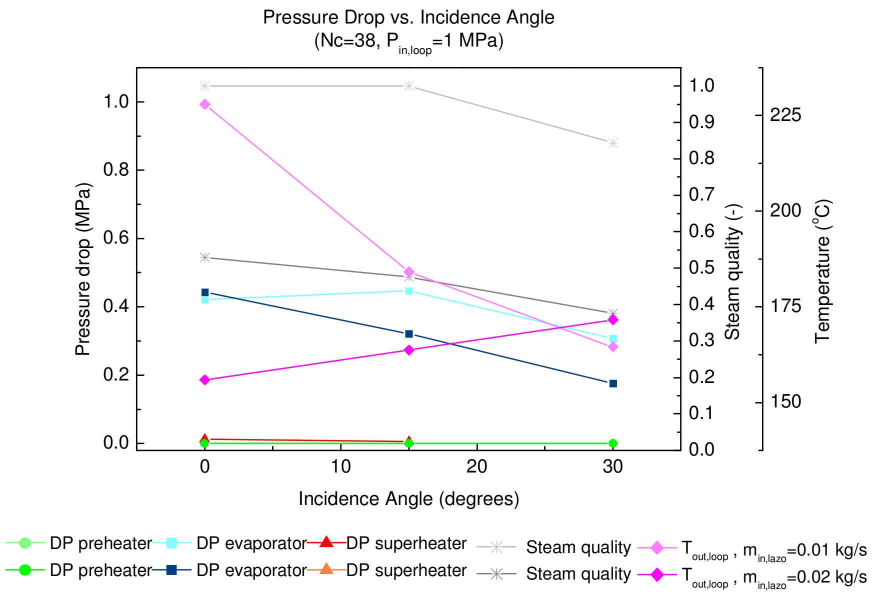

a)

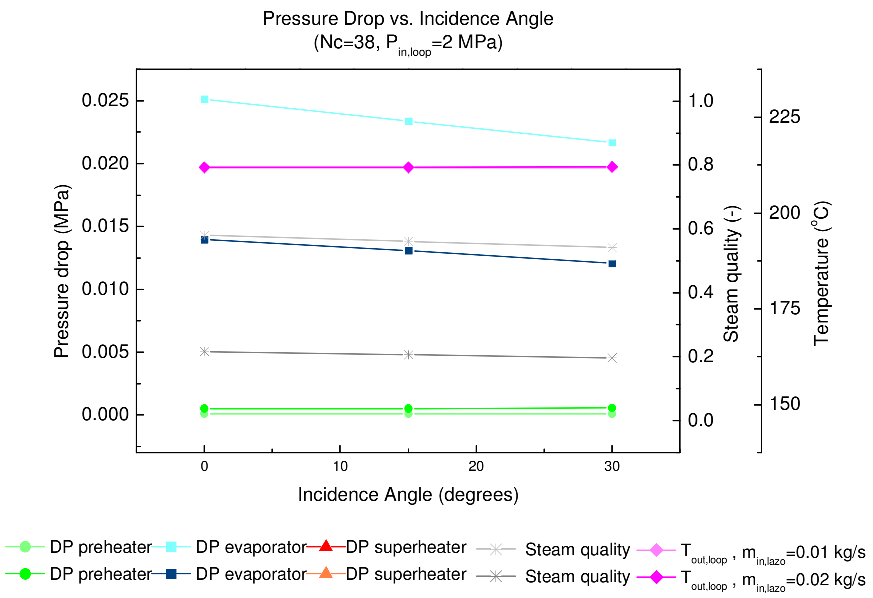

b)

Figure 5. Pressure drop versus incidence angle in the collectors' loop: a) inlet pressure of 1 MPa, b) inlet pressure of 2 MPa.

Figure 5.a) includes the results for an inlet pressure of 1 MPa. When mass flow rate is 0.01 kg/s, superheated steam appears at the outlet with incidence angles of 0º and 15º, but steam temperature varies from 228ºC to 184ºC. It is important to remark this fact because, from the operating point of view, mass flow rate should be varied during the daily operation to maintain constant the outlet steam temperature according to the process heat demand. Incidence angles for solar fields North-South oriented could vary more than 15º even for latitudes near the equator. When incidence angle is 30º, steam fraction drops to 0.84 and outlet water-steam temperature is 165ºC. Pressure losses in the evaporation section are maximum, 0.45 MPa, for an incidence angle of 15º; for incidence angle of 0º, pressure losses are 0.42 MPa, and for incidence angle of 30º, pressure losses in the evaporation section are 0.31 MPa. When mass flow rate is 0.02 kg/s, outlet steam fraction varies from 0.53 for 0º to 0.38 for 30º. Pressure losses are 0.44 MPa for the lowest angle and 0.18 MPa for the highest angle. It makes outlet water-steam temperature be higher for the highest incidence angle.

Figure 5.b) includes the results for an inlet pressure of 2 MPa. For this working pressure, differences in the results obtained for the two mass flow rates considered are only relevant regarding outlet steam fraction achieved, but pressure losses are quite small compared to the working pressure and therefore outlet water-steam temperature is maintained at 212ºC when incidence angle varies from 0º to 30º.

Table 7 compiles the data obtained when simulating the influence of the incidence angle in pressure losses.

Tab. 7: Pressure drops in the preheating, evaporation and superheating sections of the collectors' loop, outlet steam fraction and outlet fluid temperature as a function of the incidence angle of solar radiation in the Capsol-PTC collectors' loop

P_{in} (MPa)	θ (º)	ΔP_{pre} (MPa)	ΔP_{eva} (MPa)	ΔP_{sup} (MPa)	X_{out} (-)	T_{out} (ºC)	ΔP_{pre} (MPa)	ΔP_{eva} (MPa)	ΔP_{sup} (MPa)	X_{out} (-)	T_{out} (ºC)
		$\dot{m}_{in}$ =0.01kg/s					$\dot{m}_{in}$ =0.02 kg/s				
1.0	0	3E-5	0.4212	0.0121	1.00	228	0.0002	0.4431	-	0.53	156
	15	3E-5	0.4476	0.0061	1.00	184	0.0002	0.3208	-	0.48	164
	30	3E-5	0.3074	-	0.84	165	0.0002	0.1758	-	0.38	172
2.0	0	6E-5	0.0294	-	0.61	212	0.0004	0.0188	-	0.25	212
	15	6E-5	0.0247	-	0.56	212	0.0004	0.0158	-	0.22	212
	30	7E-5	0.0162	-	0.46	212	0.0005	0.0109	-	0.17	212

3.5. Producing saturated water at the collectors' loop outlet.

For the analysis presented in this section, two inlet fluid pressures, 1.0 MPa and 2.0 MPa, and two feed water temperatures, 90ºC and 125ºC, were considered. Considering these values, for each feed water pressure-temperature combination, it was calculated the minimum mass flow rate to get saturated liquid water at the collectors' loop outlet, i.e. steam fraction equal to 0 but water temperature equal to saturation temperature at the pressure calculated at the outlet. Once this minimum mass flow rate was calculated, simulations were run considering other three mass flow rates for the same set of inlet pressure and temperature. The mass flow rate values for the pair 1 MPa-90ºC are 0.08 kg/s, 0.1 kg/s, 0.12 kg/s, and 0.14 kg/s. For the couple 1 MPa-125ºC, the mass flow rates analyzed are 0.13 kg/s, 0.15 kg/s, 0.17 kg/s, and 0.19 kg/s. For the pair 2 MPa-90ºC, mass flow rates are 0.05 kg/s, 0.07 kg/s, 0.09 kg/s, and 0.11 kg/s. And finally for the pair 2 MPa-125ºC, the mass flow rate values are 0.07 kg/s, 0.09 kg/s, 0.11 kg/s, and 0.13 kg/s.

Figure 6 shows the simulation results. Observing in detail the graph, it can be seen that pressure losses in the collectors' loop follow a curve that could be adjusted to a growing exponential curve to calculate pressure losses in the collectors' loop designed as a function of mass flow rate, when at the collectors' loop outlet the subcooled-water temperature is close to saturation temperature. The evolution of the outlet temperature is just the opposite one, for higher mass flow rates water temperature decreases following a curve that could be adjusted to an exponential decay when inlet water temperature is the same, but even changing inlet water pressure.

Pressure losses in all cases are significantly lower than those obtained in previous case studies with lower mass flow rates (pressure losses are ten times lower or even less).

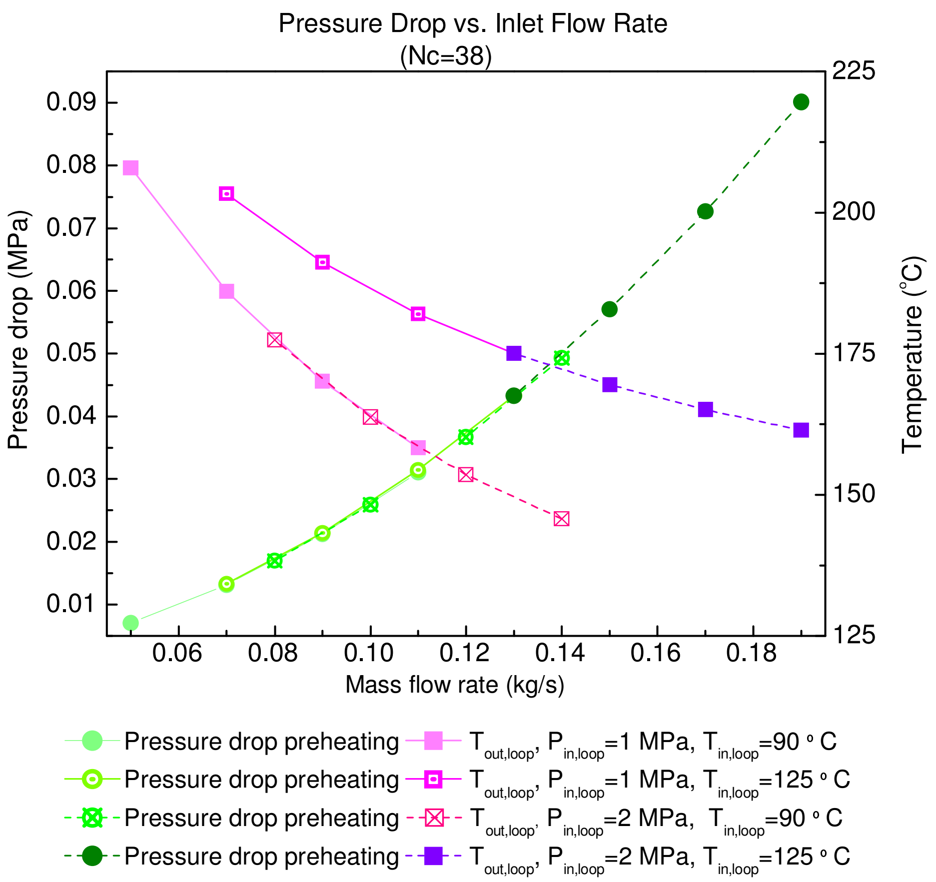

Figure 6. Pressure drop and saturated outlet water temperature versus mass flow rate .

Tab. 8: Pressure drops in the collectors' loop and outlet saturated water temperature as a function of the inlet water mass flow in the Capsol-PTC collectors' loop

P_{in} (MPa)	$\dot{m}_{in}$ (kg/s)	ΔP_{pre} (MPa)	T_{out} (°C)	$\dot{m}_{in}$ (kg/s)	ΔP_{pre} (MPa)	T_{out} (°C)
		T_{in} =90°C			T_{in} =125°C	
1.0	0.08	0.0170	177	0.13	0.0433	175
	0.10	0.0260	164	0.15	0.0570	169
	0.12	0.0367	154	0.17	0.0726	165
	0.14	0.0493	146	0.19	0.0901	161
2.0	0.05	0.0070	208	0.07	0.0133	203
	0.07	0.0132	186	0.09	0.0214	191
	0.09	0.0212	170	0.11	0.0314	182
	0.11	0.0311	158	0.13	0.0432	175

4. Conclusions

For a specific industrial process demanding thermal energy in the temperature range up to 300ºC, the use of concentrated solar technology, in particular PTC systems, could be feasible. The use of suitable simulation tools helps to optimize the configuration of the solar fields considering the particular process heat demands and other working conditions. This is a particular relevant topic when the considered size of the PTC is relatively small (i.e. the concentrator aperture and the diameter of the absorber tube are small) and direct steam generation with a two-phase flow exists in the absorber tube. It is therefore highly recommended to perform complete numerical studies of the thermal-hydraulic behaviour of different solar field configurations.

In the study presented in this paper, the Capsol-PTC collector has been considered. The number of collectors per row in the solar field considered is 38; therefore the collectors' row length is 76m. Pressure losses obtained when inlet working pressure is 1 MPa are relevant and can jeopardize the solar field operation in steady state conditions if two-phase flow is being generated. Increasing the working pressure to 2 MPa reduces pressure losses significantly and outlet fluid temperature is maintained constant in a wide range of working conditions, even when at the outlet of the solar collectors' loop there is two-phase flow, although outlet steam fraction varies.

Simulation results explained in this paper point out the technical feasibility of using small parabolic trough collectors to produce saturated steam within a temperature range suitable for many thermal industrial processes. Pressure drops obtained from this study show that the pumping power required for the solar field is affordable, thus opening the door to the implementation of solar fields with small parabolic troughs working with direct steam generation.

Acknowledgements

The authors would like to thank the Spanish Ministerio de Ciencia e Innovación (National Plan for Scientific Research, Development and Technological Innovation, 2008-2011) for the financial support given to the GEDIVA project (ENE2011-24777).

5. References

Fernández-García, A., Zarza, E., Valenzuela, L., Pérez, M., 2010. Parabolic-trough solar collectors and their applications. Renewable and Sustainable Energy Reviews 14, 1695-1721.

Fernández, A., Zarza, E., Pérez, M., Valenzuela, L., Rojas, E., Varcárcel, E., 2010. Experimental assessment of a small-sized parabolic-trough collector. CAPSOL Project. Eurosun 2010, Graz (Austria), 2010.

Hernández Lobón, D., Valenzuela, L., Zarza, L., 2011. Tool for simulating direct steam generation in parabolic Troughs. SolarPACES 2011 – Concentrating Solar Power and Chemical Energy Systems, Granada (Spain), 2011.